Pergamon

Scripta Materialia, Vol. 39, No. 3, pp. 329–334, 1998
Elsevier Science Ltd

1359-6462/98 $19.00 + .00

PII S1359-6462(98)00159-6

# INFLUENCE OF STRUCTURAL RELAXATION AND PARTIAL DEVITRIFICATION ON THE CORROSION RESISTANCE OF $Fe_{78}B_{13}Si_9$ AMORPHOUS ALLOY

C.A.C. Souza, F.S. Politi and C.S. Kiminami
Department of Materials Engineering, Federal University of São Carlos,
13569–905, São Carlos, SP, Brazil

(Received February 26, 1996)
(Accepted May 5, 1998)

## Introduction

Amorphous alloys obtained by rapid solidification from the melt exhibit a similar structure to those observed in the liquid state, i.e. without long range ordering, in such a way that the constituents of the alloy usually are randomly and homogeneously distributed. Amorphous alloys, depending on their composition, may exhibit interesting characteristics such as very soft magnetic properties and improved resistance to corrosion (1). The high corrosion resistance of these alloys is attributed mainly to a higher rate of dissolution of passivating elements in the amorphous state. In addition, amorphous alloys are chemically homogeneous and free of defects such as grain boundaries, precipitates and segregation, which are favorable sites for corrosion (1). The corrosion resistance of amorphous alloys also depends on their thermal history. Several authors (2, 3, 4) have reported that structural changes, such as structural relaxation and devitrification caused by annealing, change significantly the corrosion properties of these alloys.

The $Fe_{78}B_{13}Si_9$ commercial amorphous alloys are produced by the melt spinning process and mainly used as transformer cores owing to their excellent soft magnetic properties, but their resistance to corrosion is poor compared to other commercial amorphous alloys (5). Chattoraj et al. (6) report significant degradation of the magnetic properties caused by corrosion, and conclude that this fact must be taken seriously since, in normal applications, this alloy can rarely be isolated from corrosive agents in the atmosphere. The purpose of this paper is to study corrosion resistance of the amorphous FeBSi alloy and the effects of structural changes such as structural relaxation and partial crystallization caused by annealing.

## Experimental Procedure

$Fe_{78}B_{13}Si_9$ amorphous ribbon of 10 $\mu$m thickness and 50mm width (METGLAS 2605S-2$^{TM}$) was supplied by Allied Signal Inc., USA. Samples were studied in the as cast and annealed states. The annealing was conducted under an argon atmosphere by heating and cooling the samples at 30 degree/min. The annealing temperatures were 430, 470 and 500°C, which were selected on the basis of devitrification curves obtained by differential scanning calorimetry (DSC).

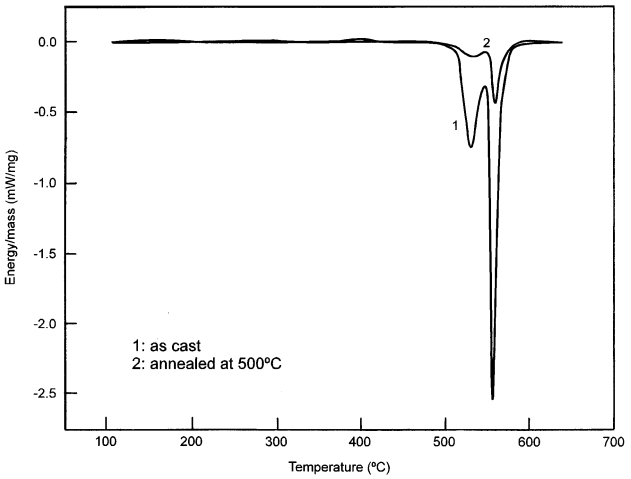


Figure 1. DSC-curves for the as-cast sample (1) and 500°C annealed sample (2).

Structural changes were characterized by DSC and X-ray diffraction (XRD). Structural relaxation in the amorphous state was monitored by measuring the apparent specific heat of both the as-cast and annealed samples by DSC in an argon atmosphere, using a heating rate of 20 degree/min.

Corrosion resistance evaluations were carried out in 0.1M $H_2SO_4$ electrolyte, using both mass loss and electrochemical measurements. Mass loss experiments were performed on $20 \times 30 \times 0.010$ mm samples with cycles of 15 minutes in the electrolyte solution. Before each weighing the samples were rinsed with carbon tetrachloride and carefully dried. The electrochemical measurements, including the charge transfer resistance, $R_{tc}$, and corrosion current density, $I_{corr}$, were taken in a three-electrode cell using a 0.62 $cm^2$ area of the bright face of the amorphous alloy ribbons as the working electrode. The auxiliary electrode was a Pt foil and a saturated calomel electrode (SCE) was used as a reference. $R_{tc}$ was evaluated by electrochemical impedance spectroscopy, EIS, at frequencies ranging from 20,000 to 0.01 Hz. The $R_{tc}$ data fitting was performed using the program "Equivalent Circuit V.3.97" written by B. A. Boukamps. The $I_{corr}$ was evaluated from potentiodynamic polarization curves, PPC, obtained with a scanning rate of 1 mV/s. The $I_{corr}$ data fitting was performed using the program "Soft.Corr - Corrosion Measurements Software, model 342." The instrumentation consisted of an EG & G PARC mod. 273 potentiostat for potentiodynamic polarization curves (PPC), and an EG & G PARC mod. 273 potentiostat and a Solartron FRA mod. 1255 for electrochemical impedance spectroscopy (EIS) measurements.

## Results and Discussion

Figure 1 shows the DSC measurements for the as-cast and 500°C annealed samples. The as-cast sample shows two exothermic crystallization peaks. The annealing at 500°C caused partial devitrification, as observed in the DSC curve with its first exothermic peak almost fully suppressed.

Figure 2 shows the XRD patterns for the as-cast and for the partially crystallized samples. The XRD of the as-cast sample exhibits only diffuse diffraction halos as is typical for amorphous alloys while the XRD of the annealed sample shows well defined peaks. Annealing at 430°C or 470°C caused only structural relaxation in the amorphous structure. The full amorphous state was preserved, as was verified by XRD and DSC analyses. DSC analyses consisted of comparing the crystallization enthalpy

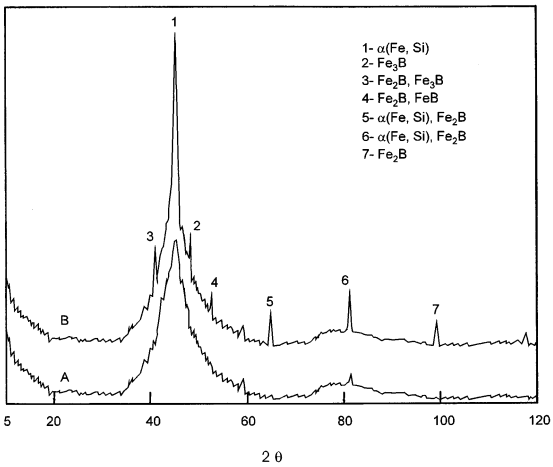


Figure 2. XRD patterns for the as-cast sample (A) and 500°C annealed sample (B).

with that for the as-cast sample. Structural relaxation was observed by monitoring the evolution of the apparent specific heat (Cp) with temperature, in both the as-cast and annealed samples. Figure 3 shows this evolution for both as-cast and 430°C and 470°C annealed samples. While the apparent specific heats of the annealed samples increase with increasing temperature, and show single endothermic peaks associated with magnetic transitions, the as-cast sample shows two endothermic peaks. This difference indicates that the annealed samples have a relaxed structure, since the first peak for the as-cast sample is related to structural relaxation. Thus as the temperature rises, the specific heat of the unrelaxed amorphous sample increases monotonically until the atoms reach a temperature at which they begin to relax. As this process involves heat liberation, the apparent specific heat starts to decrease (first endothermic peak), until the temperature reaches a point at which no further atomic rearrangements can

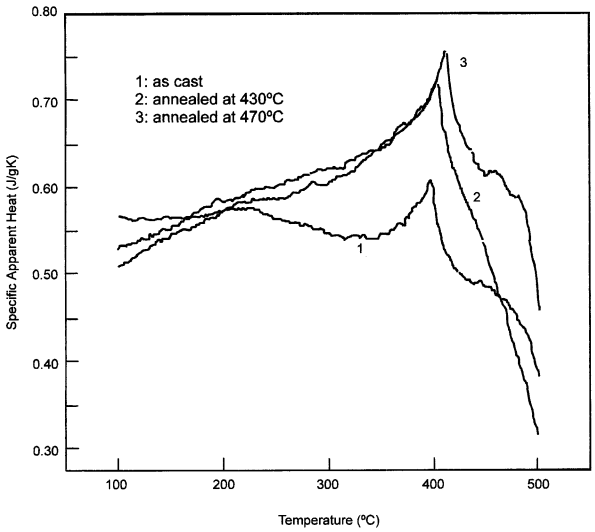


Figure 3. Evolution of the apparent specific heat with temperature for as-cast and annealed samples.

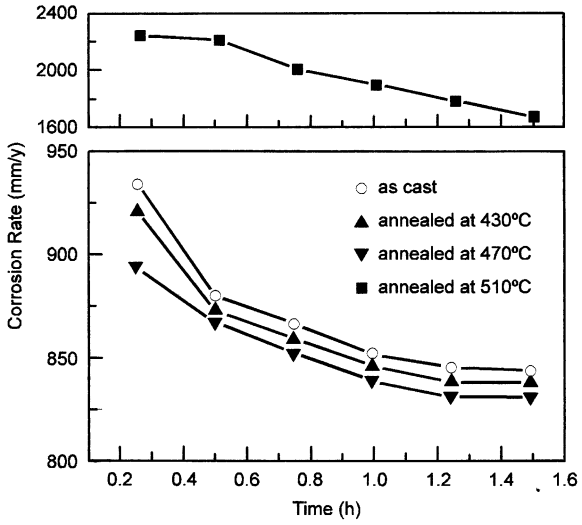


Figure 4. Values of corrosion rate obtained by mass loss experiments for as-cast and annealed samples.

occur. At this point the apparent specific heat starts to increase again until the material reaches the magnetic transition, or Curie, temperature.

Figure 4 shows the corrosion rates obtained by mass loss experiments, for the as-cast and annealed samples, and Figure 5 shows the values of charge transfer resistance, $R_{tc}$, for these samples. The corrosion density currents ($I_{corr}$) obtained from potentiodynamic polarization curves are presented in Table 1.

Samples annealed at 500 °C exhibit higher corrosion rates (mm/y) and corrosion current density, and a lower ion flux resistance ($R_{tc}$) at the metal/electrolyte interface, compared to the other samples. These results indicate that partial devitrification causes a significant decrease in the corrosion resistance of this alloy. The same effect was reported for several alloys, including both high corrosion resistance amorphous alloys with high concentrations of strongly passivating elements such as chromium (2), and other commercial alloys with lower corrosion resistance (4). This effect is attributed to microstructural

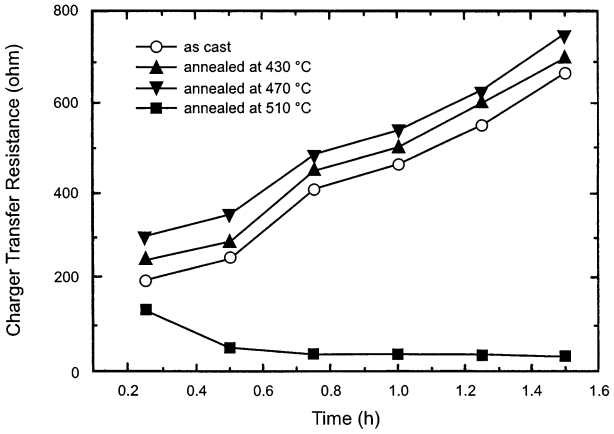


Figure 5. Values of Charge Transfer Resistance, $R_{tc}$, for the as-cast and annealed samples.

TABLE 1
Corrosion Density Currents ($I_{corr}$) Obtained From Potentiodynamic Polarization Curves, Using 0.1M $H_2SO_4$ as Electrolyte

| Sample | $I_{corr}$ [mA] |
|---|---|
| as cast | 178.8 |
| annealed at 430°C | 158.5 |
| annealed at 470°C | 151.6 |
| annealed at 500°C | 254.4 |

features such as grain boundaries, precipitates and segregation, which are favorable sites for corrosion (1) because they act as anodic regions, causing preferential etching, while the adjacent amorphous matrix acts as the cathodic region. Recently (7) it was reported that although a nanocrystallized $Fe_{78}B_{13}Si_9$ alloy has better oxidation resistance than the amorphous state, a coarse-grain crystallization leads to a deterioration in that property.

Comparing the samples annealed at 430 and 470 °C with the as-cast sample, the annealed samples exhibit lower corrosion rates (mm/y) and corrosion current density ($I_{corr}$) and a higher ion flux resistance ($R_{tc}$), indicating a higher corrosion resistance in these samples. This result may be attributed to the structural relaxation and stress relief caused by annealing. Structural relaxation decreases the free energy of the amorphous system, thereby causing a decrease in the reactivity of its elements and increasing the alloy's chemical stability. The lower corrosion rate and $I_{corr}$ and higher $R_{tc}$ of samples annealed at 470°C, compared to samples annealed at 430°C, indicate that the higher temperature annealing results in greater structural relaxation, thereby increasing the corrosion resistance.

It is also important to mention that the stress relief and structural relaxation caused by annealing treatment at 430 and 470°C can improve the soft magnetic properties of the amorphous sample. During the quenching process used to obtain the amorphous ribbons, internal stresses caused by inhomogenous quenching are formed. These stresses are a barrier for magnetic wall movement (8), and cause a lowering of magnetic performance under oscillating magnetic fields. Therefore, the stress relief improves the soft magnetic properties. The structural relaxation, which allows rearrangements in the amorphous matrix structure, such as chemical and topological short range ordering, can improve soft magnetic properties and also stability over a long period of time (9).

The increase in corrosion resistance of the alloy analyzed in this study is in agreement with results published in the literature for other magnetic soft amorphous alloys, such as FeBSi (6) and FeNiSi (4) alloys. It was reported that an increase in corrosion resistance of these alloys by annealing was achieved below the crystallization temperature, although no structural characterization of the samples was done.

## Summary

Partial crystallization of the $Fe_{78}B_{13}Si_9$ amorphous alloy caused a significant decrease in its corrosion resistance. Structural relaxation, demonstrated by the evolution of the apparent specific heat, leads to higher charge transfer resistance values and lower corrosion density current values, indicating an increase in the corrosion resistance of this alloy.

## Acknowledgments

The authors are indebted to Dr. R. Hasegawa of Allied Signal Inc. for supplying the amorphous ribbon. C.A.C. Souza is grateful to the CNPq for the award of a fellowship. The authors would like to thank the Research Foundation of São Paulo State (FAPESP)—"Projeto Temático" and Ministry of Science and Technology (MCT)—"PRONEX 1997" for financial support.

## References

1. K. Hashimoto, in Passivity of Metals and Semi-Conductors, ed. M. Froment, p. 235, Elsevier Science Publishers, Amsterdam (1983).
2. S. J. Thorpe, B. Ramaswami, and K. T. Aust, J. Electrochem. Soc. 135, 2723 (1988).
3. J. Crousier, K. Belmokre, Y. Massiani, and J. P. Crousier, in Passivity of Metals and Semiconductors, ed. M. Froment, p. 317, Elsevier Science Publishers, Amsterdam (1983).
4. V. S. Raja, K. Kishore, and S. Ranganathan, in Proceedings of the International Conference on Rapidly Quenched Metals, ed. S. Steeb and H. Warlimont, p. 1485, Elsevier Science Publishers, Amsterdam (1985).
5. I. B. Singh, T. K. G. Namboodhiri, and R. S. Chaudhary, J. Mater. Sci. 22, 2723 (1987).
6. I. Chattoraj, A. K. Bhattamishara, and A. Mitra, Scripta Metall. Mater. 26, 1013 (1991).
7. L. S. Sun, S. Shouxin, Z. Qishan, and W. Zhongguang, Scripta Metall. Mater. 32, 517 (1995).
8. D. Martinez, J. Rivas, and F. Walz, J. Non-Crystalline Solids. 156, 340 (1993).
9. Z. Kaczkowsk and L. Malkinski, J. Magnetism Magn. Mater. 83, 365 (1990).